



**JFSA**

Journal of Futuristic Sciences and Applications  
Vol. 3(2), Jul-Dec 2020, pp. 39-45  
doi: 10.51976/jfsa.322004  
www.gla.ac.in/journals/jfsa  
© 2020 JFSA, GLA University

## **Compounds of Hydroxypropyl Methylcellulose with Carbon Nanotubes: Synthesis and Analysis**

*Ashish Kumar Srivastava\* and Ankit Pratap\*\**

---

### **ABSTRACT**

*The business has developed an interest in aqueous injectable, undisturbed gel-forming solutions with a range of properties, particularly in the field of tissue engineering. In-situ gel-forming matrix may be injected into the afflicted regions without the need for surgery. Second, it may be introduced as growth factors and medications by just mixing them together, without any issues with the leftover solvents that are often used in scaffolds, and it quickly adapts to the environment after being introduced. As a result, multi-walled carbon nanotubes that had undergone acid functionalization had their carbon nanotubes oxidised before being covalently grafted onto hydroxypropyl methylcellulose (HPMC). This was accomplished by dispersing acyl-chlorinated carbon nano-tubes in HPMC after they had been treated with thionyl chloride to produce a composite material known as M. The composites are more thermally stable than their separate components, according to investigations using thermogravimetrics, FT-IR, scanning electron microscopy, and electron microscopy.*

**Keywords:** TGA; SEM; TEM; CNT; MWCNTs; HPMC; FT-IR

---

### **1.0 Introduction**

Because at least one of the stages in the composite has dimensions in the nanoscale range (1 nm = 10<sup>-9</sup> m), as described in [1,] nano-composites are so-called. They are exceptional materials with extraordinary design potential and unexpected property combinations. Their latent potential is astounding to the point that they are beneficial in a few diverse industries, spanning from manufacturing to biomedical application, with a predicted annual growth rate of roughly 25% and the fastest need to be in thermoplastic and elastomers [2]. The mechanical properties of graphene have shown that they are crucial for improving the general features of polymer nano-composites, which may be used in a range of applications [3]. Due to its adaptability, graphene has promise in a variety of industries. Even though they are good for the environment, nano-composites in the modern day provide new innovation and economic opportunities for all industries [4]. To further classify nano-composite materials, the three categories listed below may be applied. In the case of micro-composites, the matrix materials present dictate these classifications. Ceramic Matrix Nano-composites (CMNC), Metal Matrix Nano-composites (MMNC), and Polymer Matrix Nano-composites, respectively, are the names of these substances (PMNC).

---

*\*Corresponding author; Assistant Professor, Department of Mechanical Engineering, Goel Institute of Technology and Management, Lucknow, Uttar Pradesh, India (E-mail: ashishsay@gmail.com)*

*\*\*Assistant Professor, Department of Mechanical Engineering, SR Institute of Management and Technology, Lucknow, Uttar Pradesh, India (E-mail: ankitpratap.77@gmail.com)*

Although there have been a lot of studies on nano-composite systems, particularly those reinforced with CNTs, that since early 1990s, there haven't been many reviews or publications on CMNC. Carbon fiber/epoxy composites treated with AFMWCNTs distributed at a concentration of just 1% in the matrix saw increases in their Young's modulus and tensile strength of 49 and 52 percent, respectively. ILSS and flexural strength increased by 37 and 38 percent, respectively, in MMNC [5-8] and ILSS [9]. Despite this, it is important to consider the opportunities and challenges in creating structural and functional fibre nano-composites [12, 14] as well as processing, conducting, and biodegradable polymer-based mechanisms [10-12], fibre reinforced [4, 6], and morphology/property/structure aspects [5, 11-13]. In order to generate a CNT-reinforced carbon fibre nano-composite, this research team employed grey relational analysis to build a multi-objective optimization method for changing the machining settings of a die-sinking electro - discharge machine (EDM) [15]. Polymer materials are often used in industry because of their advantageous qualities, including their low weight, flexibility, and ease of fabrication. The potential of CNTs as a collection of biological applications, however, is still little understood after decades of research, posing significant obstacles and possibilities for the system.

In this work, we used MD simulations to look at what would happen if we added functionalized graphene to the cross-linked epoxy resin LY 556. The addition of graphene was made. The experiment used three distinct cross-linked epoxy solutions, two of which included graphene with various functional groups (NH<sub>2</sub>-graphene and COOH-graphene), and the third containing pure graphene [17]. The biodegradability of a given material may be greatly improved by using one of the various polymer resins available. For this particular nano-composite, hydroxyl-propyl methylcellulose (HPMC) was used as the matrix material. One cellulose ether derivative is hydroxyl-propyl methylcellulose, or hydro-mellose (HPMC). Created by reacting alkali-treated cellulose with methyl chloride and propylene oxide. Hydroxypropyl methylcellulose is another name for hydro-mellose. To be extremely biocompatible, non-toxic, and absorbable [18], they are semi-synthetic polymers of a viscoelastic nature. This study looked at how AF-MGLs impacted the tensile properties, strength, and glass transition of AF-MGL/EpC nanocomposites. In this study, the amount of AFMGLs mixed into the epoxy matrix ranged from 0% to 6% by weight. [19]

## **2.0 Composites**

### **2.1 Materials**

MWCNTs with the following properties were synthesised using the CVD method specified in the protocol using a Fe-Mo/MgO catalyst produced by the combustion technique: purity better than 98 percent, length more than 50  $\mu\text{m}$ , and diameter between 20 and 40 nm. hydroxy-propyl methylcellulose; original concentrations of nitric acid, sulphuric acid, and thionyl chloride; supplied by Thomas Backer, Mumbai.

### **2.2 Standards and tools**

Perkin-Elmer FT-IR (spectrum-1) spectrometer in KBr pellets mode (0.0051 gm of samples with 0.1 gm KBr) To verify the functional groups present in Hydroxypropyl methylcellulose and its derivatives, we have used Scan No. 36 (2  $\text{cm}^{-1}$  resolution) in the wavelength range of 400-4000  $\text{cm}^{-1}$ . A combination of freeze-dried samples and KBr is used to create pellets. Thermogravimetric analysis analyzer (TGA) SDT Q600 and Universal V4.1D TA were used for the thermal stability study. At a steady pace of 20°C/min, runs were performed between 30 and 800 degrees Celsius. In addition, a 60

ml/min nitrogen flow rate is maintained and used for conservation purposes. Scanning electron microscopy (SEM) pictures were obtained using a JEOL 2010 microscope operating at 20.0 kV; SEM images are created from a thin film that is distributed in an ethanol solution on a holey carbon grid. Transmission Electron Microscopy (TEM) at 200 kV was carried out using a Philips CM200 microscope. Drops of the sample suspension (ground in a mortar and suspended in ethanol) are being examined for characterisation of CNTs using a CM200 Philips microscope on a holey carbon grid.

### 2.3 CNT extraction and synthesizing

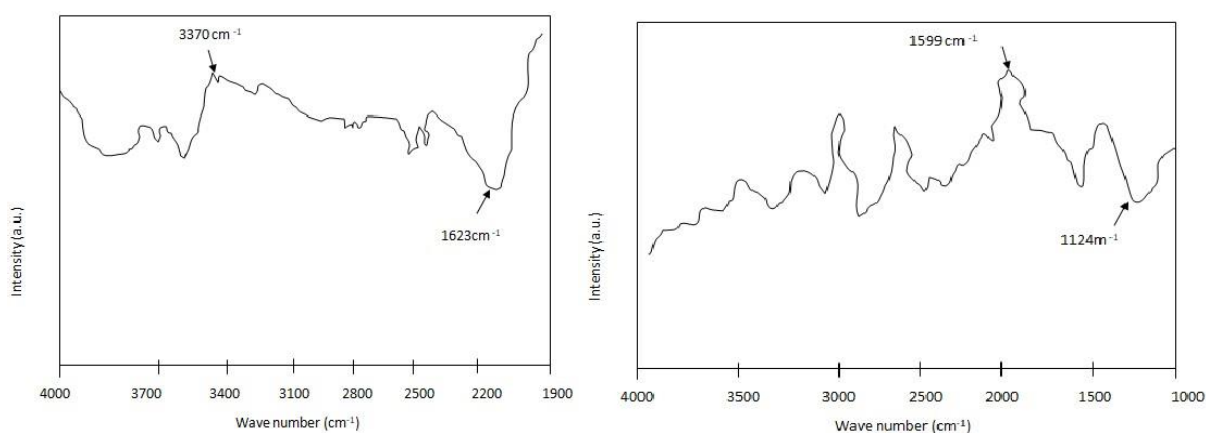
By stoichiometrically combining  $\text{Fe}(\text{NO}_3)_3 \cdot 9\text{H}_2\text{O}$ ,  $(\text{NH}_4)_2\text{MoO}_7 \cdot 4\text{H}_2\text{O}$ , and  $\text{Mg}(\text{NO}_3)_2 \cdot 6\text{H}_2\text{O}$  to produce viscous precursors, PEG 200 was then added to form Fe-Mo/MgO catalysts using the combustion method. Mixture thoroughly dissolved produces 5:0.5:70 (mass ratio). It was transferred to a silicon boat and cooked for ten minutes in a furnace at a temperature to  $550^\circ\text{C}$ . The foamy substance was ground into a fine powder once the boat cooled. In a quartz boat, 200 mg of Fe-Mo/MgO catalyst was cycled for 30 minutes while 99.9% pure  $\text{N}_2$  gas flowed through it at 140 ml/min.  $800^\circ\text{C}$  was the reaction temperature.  $\text{N}_2$  gas flow rate was regulated at 140 ml/min while 99.99 percent pure acetylene gas was delivered into the reaction chamber at a rate of 60 ml/min for 30 minutes. Under  $\text{N}_2$  atm, the furnace cooled down. Black powder found in the quartz boat sample. Samples underwent two filters. I avoided using MgO support when immersed in 36 percent HCl and vibrating ultrasonically for 30 minutes. fluid from a centrifuged supernatant. (ii) Gas oxidation at  $500^\circ\text{C}$  was used to eliminate amorphous carbon. Pre- and post-purification examination of carbon deposits: Carbon yield is equal to (weight lost during carbon oxidation minus residue after oxidation) \*100%. This method produces CNTs that are 98 percent pure.

## 3.0 Results and Discussion

### 3.1 FT-IR analysis

When determining the kind of chemical bonding, infrared (IR) spectroscopic is often employed. If clean bonds were formed, it will be easy to tell by comparing the infrared spectra of CNTs during functionalization. We crushed pellets of nanostructured Materials (CNT-COOH, CNT-COCl, and Carbon nanotube composite) as well as pellets of pure CNTs using KBr powder, and then we acquired the spectra of these materials (Fig. 1).

**Figure 1: The FT-IR spectra of composite CNT made of (a) pure CNT, (b) CNT-COOH, (c) CNT-COCl, and (d) CNT-HPMC.**



The peak at 3370 cm<sup>-1</sup> caused by intermolecular H-bonded O-H stretch has a lesser absorption before to acid oxidation (Fig. 1(a) and (b)), but after acid oxidation, it changes into an incredibly wide and robust absorption peak. The weaker signal at 1623 cm<sup>-1</sup> is related to the absorption of the carbonyl group when it is coupled with an olefinic (C=C-C=C) double bond.

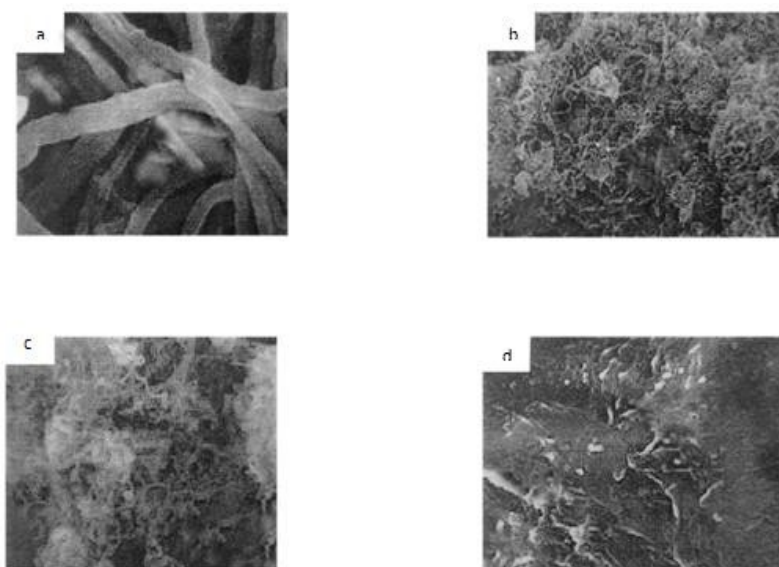
During thionyl chloride processing with CNT-COOH, the large region between 850 and 550 cm<sup>-1</sup> due to C-Cl extending vibration confirms the existence of -COCl, and the presence of the -Cl group with -C=O has indeed been verified by 1657 cm<sup>-1</sup> [Fig. 1(c)]. [Note: 1657 cm<sup>-1</sup> has given credit for the existence of the -Cl grouping with -C=O.] Due to substantial hydrogen bonding and a minimal energy shift in the -C=O extended to 1599 cm<sup>-1</sup>, the 3451 cm<sup>-1</sup> peak is noticeably enlarged in the CNT-HPMC. Both of these elements had a role in the peak's expansion. According to Fig. 1(d), the peak deduced from B (1,4) glycosidic linkages and the C-O-C prolonged vibration were both moved to 1124 cm<sup>-1</sup>.

### 3.2 Assessment of electron microscopy

SEM analysis has revealed information on the sizes and shapes of the functionalized, purified CNTs. The SEM picture of pure CNTs (Fig. 2(a)) shows the CNTs to be uniformly oriented and free of flaws. The nano-tubes may be several micrometres in length and have diameters ranging from 20 to 41 nm, although some are curved.

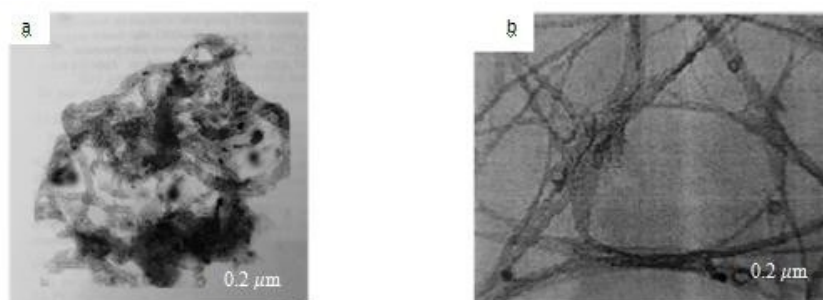
SEM was also employed to examine the carbon nano-tube sample following alteration with -COOH, -COCl and Hydroxy propyl methylcellulose. As illustrated in Fig. 2(b) the shape of carbon nano-tubes following oxidation with acids is retained. Some breakdown was seen, suggesting that the carbon nano-tubes were dissolved by the powerful acids. The SEM of CNT-COCl reveals the presence of CNTs in micron length (fig.2c) and the bond formation with hydro-mellose (HPMC) of functionalized CNTs (fig.2d); additionally, the surface texture of CNT-HPMC reveals the presence of a distinct agglomeration of CNTs within the regions of HPMC in which it has been cloistered, suggesting the existence of a more hydrophobic phase.

**Figure 2: SEM images of CNT-COOH, CNT-COCl, and a Composite of CNT and HPMC in (a) pure MWNTs, (b) CNT-COOH, and (c) CNT-COCl**



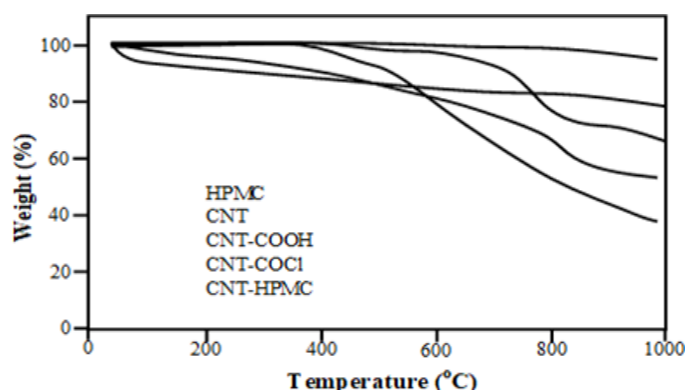
Coatings on CNTs are readily apparent in transmission electron microscopy (TEM) (Fig. 3b) images of Hydroxypropyl methylcellulose on CNTs and CNT-COCl. Significant analysis showing that functionalized CNTs have incorporated into the surface of HPMC.

**Figure 3: TEM Images of CNT-COCl (a) and CNT-g-HPMC (b)**



### 3.3 Thermal assesment

**Figure 4: TGA Examination**



The temperature performance of CNT and CNT-HPMC compounds is shown in Figure 4. At 800 °C, the weight loss of as-blended CNTs was less than 1%, demonstrating the immaculateness and lack of defects in the nanotubes. More abnormalities were produced by the acid oxidation of CNTs, which contain COOH functional groups. At 800°C, it showed a full weight decrease of around 50%. With things aside, corrosive oxidation using intense H<sub>2</sub>SO<sub>4</sub>/HNO<sub>3</sub> mixtures also resulted in CNTs being cut and the development of further abnormalities where they were. It is clear that the weight decrease is halved at 800°C. Thermal analysis of pure HPMC shows two specific weight losses below 450 °C. The methyl and propyl side groups are involved for the HPMC's 20 % weight loss. Therefore, it is highly likely that the thermal stability of HPMC has improved in the presence of CNTs. It has been suggested that the second weight loss occurred between 600 and 800°C and was caused by the oxidative ejection of glycosidic linkage.

### 4.0 Conclusion

Based on functionalized MWCNTs, a very effective drug delivery method has been developed. The restrictions of the CNT-based systems were overridden and eliminated by this

technology. Covalent characterization of CNT-HPMC has been used in order to produce nanotubes. CNTs were incorporated into HPMC, which enhanced the material's thermal properties. For validation, the bond involving CNTs and HPMC was investigated using FTIR, SEM, and TEM. The capacity to control the dosage of medication to be used for drug delivery as well as a reduction in toxicity, which helps patients experience fewer side effects, are both research goals in the following phase of the study. Additionally, it is feasible to investigate and enhance the process by which unprocessed MWNTs may be converted into new derivatives thanks to the connections of HPMC group on the caps and wall of MWNTs. A variety of medical applications for a variety of industries may be produced by manipulating CNT materials.

## References

- [1] Roy.R, Roy. R.A, Roy.D.M. "Alternative perspectives on "quasi-crystallinity": non-uniformity and nanocomposites", *Mat. Let.* Vol.4:1986; pp323-328.
- [2] Iijima.S. "Helical microtubes of graphitic carbon", *Nature.* Vol.354:1991;pp56-58.
- [3] A Kumar, K Sharma, AR Dixit A review of the mechanical and thermal properties of graphene and its hybrid polymer nanocomposites for structural applications, *Journal of materials science* 54 (8), 5992-6026
- [4] Choa.Y.H, Yang.J.K, Kim.B.H, Jeong.Y.K, Lee.J.S, Nakayama.T et al. "Preparation and characterization of metal: ceramic nanoporous nanocomposite powders", *J. Magnetism and Magnetic Mat.* Vol. 266:2003; pp12-19.
- [5] Goyal, M. and B. Gupta, Analysis of shape, size and structure dependent thermodynamic properties of nanowires. *High Temperatures--High Pressures*, 2019. 48.
- [6] Thostenson.E.T, Ren.Z, Chou.T.W. "Advances in the science and technology of carbon nanotubes and their composites: a review", *Composites Sci. & Tech.* Vol.61:2001;pp1899-1912.
- [7] K Sharma, M Shukla, Three-phase carbon fiber amine functionalized carbon nanotubes epoxy composite: processing, characterisation, and multiscale modeling, *Journal of Nanomaterials* 2014
- [8] Peigney.A, Laurent.C.E, Flahaut.E, Rousset.A. "Carbon nanotubes in novel ceramic matrix nanocomposites", *Cer. Int.* Vol.26:2000; pp677-683.
- [9] Choi.S.M, Awaji.H, "Nanocomposites, a new material design concept", *Sci. & Tech of Adv. Mat.* Vol.6:2005; pp2-10.
- [10] Goyal, M. and B. Gupta, Study of shape, size and temperature-dependent elastic properties of nanomaterials. *Modern Physics Letters B*, 2019. 33(26): p. 1950310.

- [11] Pandey.J.K, Kumar.A.P, Misra.M, Mohanty.A.K, Drzal.L.T, Singh.R.P, “Recent advances in biodegradable nanocomposites”, *J. Nanosci. & Nanotech.* Vol.5: 2005; PP497-526.
- [12] Pokropivnyi .V, “Two-dimensional nanocomposites: photonic crystals and nanomembranes (review). II: Properties and applications”, *Powder Metallurgy and Metal Ceramics.*, Vol.41:2002; pp369-381.
- [13] Ray.S.S, Bousmina.M, “Biodegradable polymers and their layered silicate nanocomposites: In greening the 21st century materials world”, *Progress in Mat. Sci.* Vol.50:2005; pp962-1079.
- [14] Gangopadhyay.R, Amitabha.D, “Conducting polymer nanocomposites: brief overview”, *Chem. Of Mat.* Vol. 12:2000; pp608-622.
- [15] Wang.C, Guo.Z.X, Fu.S, Wu.W, Zhu.D, “Polymers containing fullerene or carbon nanotube structures”, *Progress in Polymer Science.*, Vol.29:2004;pp1079-1141.
- [16] Alexandre.M, Dubois.P, “Polymer-layered silicate nanocomposites: preparation, properties and uses of a new class of materials”, *Mat. Sci. & Engg.* Vol.28:2000; pp1-63.
- [17] K Mausam, K Sharma, G Bharadwaj, RP Singh, Multi-objective optimization design of die-sinking electric discharge machine (EDM) machining parameter for CNT-reinforced carbon fibre nanocomposite using grey relational analysis, *Journal of the Brazilian Society of Mechanical Sciences and Engineering* 41
- [18] Pandey.J.K, Reddy.K.R, Kumar.A.P, Singh.R.P, “An overview on the degradability of polymer nanocomposites”, *Polymer Degradation and Stability*, Vol.88:2005;pp234-250.
- [19] A Yadav, A Kumar, PK Singh, K Sharma, Glass transition temperature of functionalized graphene epoxy composites using molecular dynamics simulation, *Integrated Ferroelectrics* 186 (1), 106-114